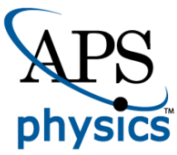

Unexpected Phenomenology in Particle-Based Ice Absent in Magnetic Spin Ice

Cristiano Nisoli

Phys. Rev. Lett. **120**, 167205 — Published 19 April 2018

DOI: 10.1103/PhysRevLett.120.167205

Spin Ice versus Thin Ice: Uncovering Novel Phenomenology in Particle-Based Ices

Cristiano Nisoli
*Theoretical Division, Los Alamos National Laboratory, Los Alamos, NM, 87545, USA**
(Dated: March 15, 2018)

While particle-based ices are often considered essentially equivalent to magnet-based spin ices, the two differ essentially in frustration and energetics. We show that at equilibrium particle-based ices correspond exactly to spin ices coupled to a background field. In trivial geometries such field has no effect and the two systems are indeed thermodynamically equivalent. In other cases, however, the field controls a richer phenomenology, absent in magnetic ices, and still largely unexplored: ice rule fragility, topological charge transfer, radial polarization, decimation induced disorder, glassiness.

Introduction. The ice rule [1] has had an impactful history. Pauling employed it to explain [2] the zero point entropy of water ice [3] as a consequence of the degeneracy in allocating two protons close to, and two away from, each oxygen atom sitting in any of the tetrahedron-based crystal structures of ice. However, the concept is more general. Consider binary spins placed along the edges of a graph, impinging in its vertices (Fig. 1). The topological charge of a vertex of coordination z is the difference between the n spins pointing in and the $z-n$ pointing out, or $q_n = 2n - z$. Then, an ice-manifold is the degenerate set of spin configurations that minimizes $|q|$ locally. If z is even, the minimal $|q|$ is zero (for $z = 4$, we recover the original ice rule, 2-in/2-out, of water ice and rare earth spin ices[4]). If z is odd, ice rule vertices have charges $q = \pm 1$ and the ice-manifold is a neutral plasma of topological charges [5–9].

As ice manifolds can typically host unusual phases [10], they have invited the design of a new class of artificial, frustrated magnetic nano-materials, called "artificial spin ices" (SI). These are arrays of interacting, single-domain, shape-anisotropic, ferroics nano-islands whose magnetizations are described by binary spins that obey the ice rule (Fig. 1a,b) [11, 12]. Their exotic behaviors are often not found in natural magnets [13] and can be designed to study memory effects [14], effective thermodynamics in driven systems [15], kinetics of magnetic charges [8, 16–18], anomalous hall effects [19, 20], often even with unprecedented real-time, real-space characterization [21–25].

"Particle ices" (PI) are another artificial implementation of an ice manifold [26–31]. Mutually repulsive particles are trapped, one particle per trap, with preferential occupation at its extremes (Fig. 1c,d). Traps are arranged along the edges of a lattice whose geometry determines the collective behavior. They have been studied numerically [26–28] and realized experimentally via colloids gravitationally trapped in microgrooves [32, 33] but also in flux quanta pinned to nano-patterned superconductors [34–36]. As PI was also found to obey the ice rule, at least in the square and hexagonal geometry, ideas and results have been exchanged among PI and SI, often considered as essentially equivalent systems.

That assumption is incorrect. Despite similarities, the two systems differ essentially in energetics and in frustration. While local energetics promotes the ice rule in SI, it opposes it in PI. The energy of a SI vertex is typically proportional to the square of its topological charge, $E \propto q_n^2$, thus favoring the ice rule. For PI, it is instead $E \propto n(n-1)$, thus favoring large negative charges which violate the ice-rule (Figs. 2, 3). In PI the ice-manifold emerges as a collective rather than local energetic compromise and only in the thermodynamic limit (see below). It is thus a locally unstable and fragile "thin ice".

We provide here a unifying framework for the complex phenomenology of similarities and differences among the two classes of materials: PI at equilibrium can be mapped directly into a SI coupled to a geometry-dependent background field. In trivial geometries this field has no effect, and the two ices are equivalent. In non-trivial ones, it mediates the breakdown of the ice rule, leading to an entirely new phenomenology, still largely unexplored. Without pretense of exhaustiveness we will suggest some implications of this mapping in terms of novel behaviors which invite further experimental exploration.

1. Isomorphism. In PI, particles in positions $\{\mathbf{y}\}$ repel with isotropic interaction ϕ. Their total energy $\mathcal{H} = \sum_{\mathbf{y}\neq\mathbf{y}'} \phi(|\mathbf{y}-\mathbf{y}'|)$ does not look conducive to SI physics. Yet, at equilibrium the position $\mathbf{y}^+$ of the particle in a trap is a binary variable, represented by —● or ●— (Fig 1c,d). We can map PI into SI by ascribing

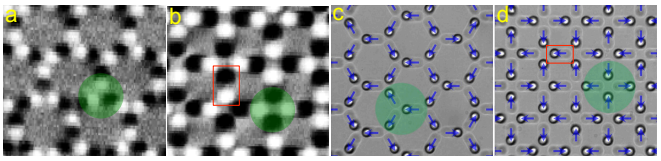

FIG. 1: Magnetic force microscopy of hexagonal (a) and square (b) SI show the constitutive degrees of freedom (red rectangles) as dumbbells of positive (white) and negative (black) magnetic charges (from [15]). Optical microscopy of hexagonal (c) and square (d) PI, where the blue arrows denote the equivalent spins $\vec{\sigma}_{\mathbf{x}}$ (from [32]). Green disks show ice rule obeying vertices, of minimal absolute topological charge.

*cristiano.nisoli@gmail.com,cristiano@lanl.gov

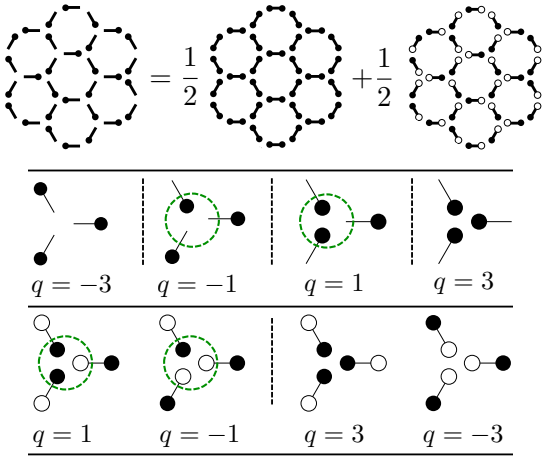

FIG. 2: Top: Schematic illustration of Eq. (1) where an hexagonal PI (here in a random configuration) is decomposed into a SI, with dipolar degrees of freedom, plus a background of positively saturated traps. The energy of the PI (middle) and SI (bottom) vertices, listed in increasing order (from left to right, separated by dotted vertical lines) differ essentially. PI promotes vertices of large negative charge, violating $\mathbb{Z}_2$ symmetry. SI promotes vertices of low absolute topological charge (ice rule vertices, circled in green have the same energy in SI but not in PI).

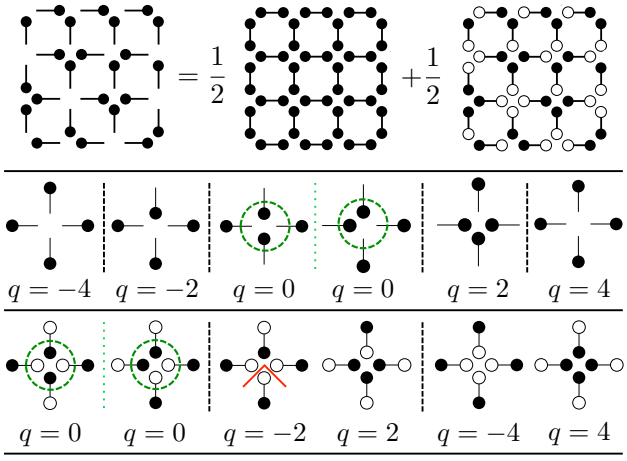

FIG. 3: Same as in Fig. 2, but for the square lattice. Here, however, the degeneracy of the ice-rule vertices ($q=0$) is lifted by a difference in interaction strength between perpendicular and collinear traps or dumbbells, and polarized vertices (middle: forth from left; bottom: second from left) have higher energy. The red $\wedge$ connects two plaquettes where the head-to-toe rule is broken by a monopole (see Fig. 5).

a *positive* charge to the real ● particles and introducing in the empty locations $\mathbf{y}^-$ of the traps virtual *negative* charges ○, which repel (attract) other negative (positive) charges. We can then fractionalize a trap on an edge $\mathbf{x}$ as

$$\text{—●} = \frac{1}{2}\,\text{●—●} + \frac{1}{2}\,\text{○—●}, \tag{1}$$

i.e. a *positive dumbbell* ●—● (a trap doubly occupied by positive charges), plus a *dipole* of negative and positive charges represented by a spin $\vec{\sigma} =$ ○—● located in $\mathbf{x}$, the center of the trap so that $\mathbf{y}^{\pm} = \mathbf{x} \pm \vec{\sigma}/2$. Then, as spins are binary, the energy can always be rewritten as

$$\mathcal{H} = \frac{1}{2}\sum_{\mathbf{x}\neq\mathbf{x}'} \sigma^i_{\mathbf{x}} J_{ii'}\left(\mathbf{x}-\mathbf{x}'\right)\sigma^{i'}_{\mathbf{x}'} - \sum_{\mathbf{x}} \vec{\sigma}_{\mathbf{x}}\cdot\vec{B}(\mathbf{x}). \tag{2}$$

The first term expresses the SI part of the hamiltonian and $J_{ii'}(\mathbf{x})$ is a tensor field that can be reconstructed from ϕ. The second term represents the interaction between dipoles and the positive dumbbells which generate the background field $\vec{B}$ (see Supp. Mat. for a constructive derivation).

We will often adopt a nearest neighbor vertex model approximation [37, 38] and consider the "vertex-energies", i.e. the interaction energies of all the spins impinging in a vertex. Figures 2, 3 show the different energy hierarchies for hexagonal and square geometries in the two pictures, where the SI picture recovers a $\mathbb{Z}_2$ symmetry absent in the PI picture.

We will call a geometry *trivially-equivalent* if $\vec{B}=0$: then PI behaves as a SI at equilibrium. Clearly that is true if a lattice has point reflection symmetry in the middle points $\{\mathbf{x}\}$ of each edge. Thus, the hexagonal and square PI follow the ice rule, as found previously numerically and experimentally [26, 27, 32, 33].

2. Ice rule and inner phases. SI often exhibits phases within its ice manifold. E.g., honeycomb SI enters a charge-ordered/spin-disordered phase within its ice manifold, and then a long-range ordered, demagnetized phase within its charge-ordered phase [5, 7–9, 39]. Following ref [40], we can perform a dipolar expansion of (2)

$$\mathcal{H} \simeq \frac{k}{2}\sum_v q_v^2 + \frac{1}{2}\sum_{\langle v,v'\rangle} q_v q_{v'}\phi(r_{v,v'}) + \frac{1}{2}\sum_{\mathbf{x}'\notin\partial\mathbf{x}} \sigma^i_{\mathbf{x}} J_{ii'}\left(\mathbf{x}-\mathbf{x}'\right)\sigma^{i'}_{\mathbf{x}'} - \sum_{\mathbf{x}} \vec{\sigma}_{\mathbf{x}}\cdot\vec{B}(\mathbf{x}) \tag{3}$$

which shows that PI also admits inner phases. The first term imposes the ice rule from the interaction among dipoles within a vertex (q_v is the charge of the vertex v, and $k>0$ depends on ϕ). The second term is an interaction between charged vertices and implies charge order at lower temperatures, as was recently seen numerically for PI with repulsion $\phi = x^{-3}$ [29]. In the third term $\partial\mathbf{x}$ is the neighborhood of $\mathbf{x}$ and J_{ij} can be obtained from ϕ by dipolar expansion. For instance, for $\phi \propto r^{-\alpha}$ we find

$$J_{ij}(\mathbf{r}) \simeq \left[\delta_{ij} - (\alpha+2) r_i r_j\right] r^{-\alpha-2}, \tag{4}$$

which reduces to the familiar dipolar interaction for $\alpha = 1$. Instead, $\alpha > 1$ in (4) strengthens the ferromagnetic

term, leading to the ferromagnetic ordering within the disordered ice-manifold which has been recently obtained numerically in hexagonal PI [29] for $\alpha = 3$. In the fourth term of (3), $\vec{B} = -\vec{\nabla}\psi$ [with $\psi(\mathbf{x}) = \sum_{\mathbf{y}_\bullet \neq \mathbf{x}} \phi(\mathbf{x} - \mathbf{y}_\bullet)$, where $\mathbf{y}_\bullet$ runs over all the allowed particle positions in all the dumbbells ●—●] is the polarizing background field, whose role in ice rule fragility we will discuss now.

3. Ice rule fragility in finite size systems. Breakdown of the ice rule in PI follows from its local energetics lacking $\mathbb{Z}_2$ symmetry. Within the SI picture, it is explained by the background field. One obvious case is a finite portion of an otherwise trivially-equivalent geometry. Then a finite chunk of positive dumbbells is the source of $\vec{B}$, which thus points toward the boundaries, polarizing the spins outwards. The consequent accumulation of positive charges on the boundaries necessarily implies a violation of the ice rule in the bulk, as the net charge of a system of dipoles is zero.

This polarization has been observed experimentally (reported to us by P. Tierno, Barcelona). Instructively, this break-down of the ice-rule disappears in the thermodynamic limit. The total negative charge in the bulk is proportional to the flux of $\vec{\sigma}_{\mathbf{x}}$ at the boundaries, and thus bound by their length L. Therefore, the surface charge density goes to zero at least as L^{-1}. The ice-rule in PI is a collective effect only recovered in the thermodynamic limit. Nothing of the sort happens in SI [41].

4. Ice rule fragility in extended systems. More interesting is the ice rule breakdown in infinite lattices that are non-trivially-equivalent, such as a (regular or random) decimation of a trivially-equivalent geometry. Because the background of *positive* dumbbells has no effect in the original, undecimated geometry, its effect in the decimated geometry can be expressed as coming from *negative* virtual dumbbells ○—○ (i.e. traps saturated with negative particles) placed in correspondence of the decimated links.

Crucially, in a vertex-model approximation the SI energy of a vertex is thus proportional to its net *virtual* charge $\tilde{q}$, inclusive of the charge of the negative, virtual dumbbell ○—○, thus breaking the $\mathbb{Z}_2$ symmetry of the SI energetics. Fig. 4 shows the case of an honeycomb ice. For $z = 2$ vertices, the ice rule violating 2-in/0-out configuration (of *virtual* charge $\tilde{q} = -1$ but *real* positive charge $q = 2$) *has the same SI energy* of the ice-rule obeying configuration of 1-in/1-out ($q = 0$, $\tilde{q} = +1$). It also of the ice rule obeying $z = 3$ vertices. Thus, $q = 2$ charges appear entropically on $z = 2$ vertices in the degenerate ground state, in violation of the ice rule. The $z = 3$ vertices remain in the ice rule, but $q = -1$ charges must exceed $q = 1$ ones, to cancel the positive charge on the $z = 2$ vertices.

This argument is completely general. Any mixed coordination lattice obtained from decimating a trivially-equivalent, ice-rule obeying PI must similarly show a transfer of topological charge from vertices of higher coordination to the decimated vertices of lower coordination, where charge is attracted by the negative virtual charges

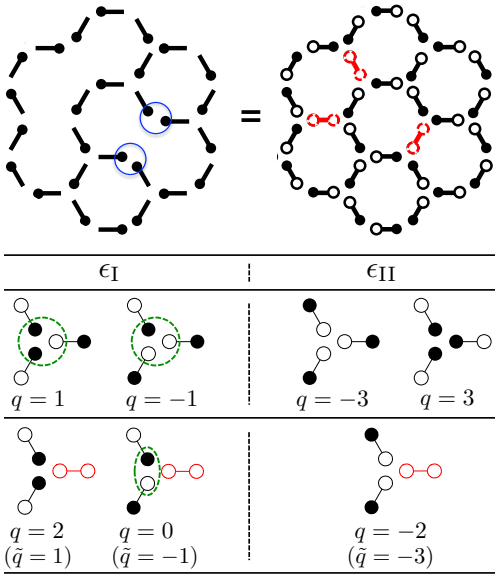

FIG. 4: A portion of a decimated, infinitely extended honeycomb PI (top left) in its low energy state can have ice rule violations on z=2 vertices ($q = +2$, blue circles) because it is equivalent to a SI stuffed with virtual, negatively saturated traps (red, dashed) in lieu of the removed links (top right) with no violations of the ice rule in the virtual charge ($\tilde{q} = \pm 1$). Indeed, while the SI energetics of the undecimated, $z = 3$, vertices (middle) is left unchanged, that of the decimated $z = 2$ vertices (bottom) must include virtual negative saturated traps, and thus violates the ice rule at lowest energy: the vertex of real charge $q = 2$ (virtual charge $\tilde{q} = 1$) is degenerate with the vertex of real charge $q = 0$ (virtual charge $\tilde{q} = -1$), and with the $z = 3$ vertices of real charge $q = \pm 1$ (ice rule vertices circled in dashed green).

that replace the decimated link. This does not imply, however, that violation of the ice rule, must necessarily happen in the lowest coordination vertices, as demonstrated below and as found recently [42] in square PI. This ice-rule violation through charge transfer is unique to PI, and nothing of the sort can happen in SI, where the ice rule is robust to decimation and mixed coordination [13, 24, 43], dislocations [44], and indeed even in clusters [41], because it is enforced by the local energy.

Finally, charge transfer should be associated with glassiness. Indeed, while the average net charge must remain zero, or $q_{\rm net} \equiv N_v^{-1} \sum_v \langle q_v \rangle = 0$ (N_v is the number of vertices), its Edwards-Anderson parameter is not, or $q^2_{\rm EA} \equiv N_v^{-1} \sum_v \langle q_v \rangle^2 \neq 0$, because of the breakdown of the $\mathbb{Z}_2$ symmetry in the equivalent PI picture. This implies freezing of the charge in random distributions as $q^2_{\rm EA}$ is also the time autocorrelation function at large times.

5. Order breakdown from topological charge transfer. It is well known that the ice manifolds of square PI (or SI) are antiferromagnetically ordered because traps (or spins) converging perpendicularly in the vertex interact more strongly than those converging collinearly. This

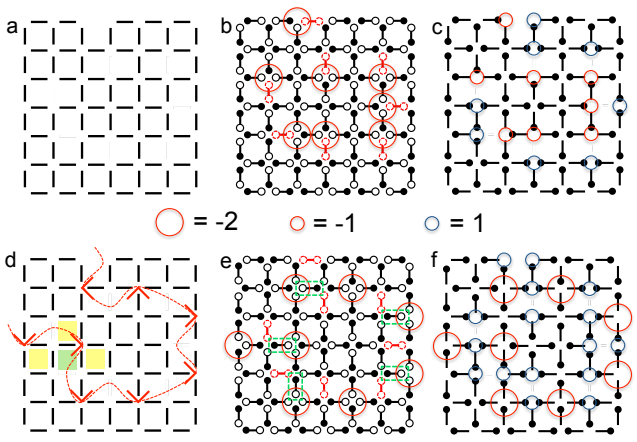

FIG. 5: Top (a-c): Decimating a square lattice (a) *and* its anfiferromagnetic ground state (decimated traps are replaced with negatively saturated traps, in red) leads to an ordered lowest energy state with $\tilde{q} = -2$ virtual charges on half of the decimated vertices in the SI picture (b). It corresponds to $q = \pm 1$ real charges on decimated vertices in the PI picture (c) and thus all vertices obey the ice rule. At low decimation, this is the only low energy state. Bottom (d-f): However, above the decimation threshold corresponding to the percolation of decimated neighboring square plaquettes [e.g. yellow shaded ones neighboring a green one in (a)], the low energy state becomes degenerate. A disordered state can be chosen by connecting (red dotted line) neighboring decimated plaquettes (d) with $q = -2$ monopoles (represented with $\wedge$ connectors as in Fig. 3) on $z = 4$ vertices, thus removing the virtual charges from decimated, $z = 3$ vertices without increasing the energy [(e), green rectangles frame spins that can be freely flipped]. In the PI picture (f) this corresponds to ice rule violations on the $z = 4$ vertices hosting charge $q = 2$: disorder comes from entropic transfer of topological charge.

lifts the degeneracy of the ice-rule and favors the non-polarized, antiferromagnetic ice rule vertices [8, 11, 23, 26, 45] of Fig. 3. Consider a random decimations of traps in square PI that does not create $z = 2$ vertices. Such decimation corresponds to a partial cover for a dimer cover model on the edges of the square lattice (Fig. 5a), and in SI it is expected to preserve the antiferromagnetic order [13]. In PI, instead, it implies a structural transition to disorder, as we show now.

Consider a spin state obtained by decimating the antiferromagnetic ensemble (Fig. 5b,c). The presence of virtual negative dumbbells creates a negative virtual monopole $\tilde{q} = -2$ on half of the $z = 3$ vertex. Because the SI energy is inclusive of virtual charges, and because of (virtual and real) charge conservation, this decimated, antiferromagnetically ordered state, which *obeys the ice rule* as $z = 3$ vertices all have charges $q = \pm 1$, Fig. 5c), has the lowest energy (at least at the vertex-model approximation). And yet, is it unique?

At sufficiently low decimation it clearly is. Indeed, in a low energy state only antiferromagnetic $q = 0$ ground state vertices, and possibly $q = -2$ monopoles are allowed on $z = 4$ vertices (corresponding to the removal of virtual charges $\tilde{q} = -2$ on decimated vertices. Therefore, in each square plaquette the four dipoles must be arranged head to toe, except in correspondence of a monopole. In a plaquette containing a virtual trap, a negative virtual charge sits on one of the two decimated vertices if and only if the remaining three spins are arranged head to toe (Fig. 5b). Antiferromagnetic order breaks down when both virtual charges on the two neighboring decimated vertices are $\tilde{q} = 0$ (and therefore their real charge is positive, $q = 1$, on both, corresponding to net positive charge transfer from $z = 4$ to$z = 3$ vertices). For that to happen, the head to toe rule must be broken on one of the two other vertices in each of the two corresponding decimated plaquettes, corresponding to two monopoles of charge $q = -2$, as monopoles are the only allowed vertices that can beak the head-to-toe rule on $z = 4$ vertices. Because a monopole breaks the head-to-toe rule on two of the four plaquettes it separates (red wedge in Fig. 3), this does not raise the energy only if at least one of the nearest neighboring plaquette is also decimated (Fig. 5d). Therefore, when the decimation is sufficiently low and the number of neighboring decimated plaquette is non-extensive the decimated antiferromagnetic state is the only ground state. However, when nearest neighboring decimated plaquette percolate (Fig. 5d), the low energy ensemble becomes disordered.

One can prove so by construction. Start with the decimated lattice, connect (or not) any neighboring decimated rectangular plaquette which can be connected via the red $\wedge$-connector of Fig. 5d, representing a monopole (Fig. 3). Then all the spins are determined. This construction corresponds to lines threading through decimated plaquettes (red dotted in Fig. 5d). When the decimated plaquettes percolate at the nearest neighbor, these lines can be chosen freely either as closed loops or as infinite paths percolating through the material. This freedom in choosing connecting lines, and more trivially the resulting free spins (Fig. 5e), give a residual entropy density to the ground state. There is thus in decimated square PI a transition from order to a disordered state at a critical decimation, likely a glassy one (see above) involving dynamic arrest, and which invites experimental analysis. Interestingly, it corresponds to a specific percolation threshold for a dimer cover model.

Finally, note that below that structural transition, while the ground state remains unique, its excitation profile might change with decimation in ways not yet understood, making the antiferromagnetic order more fragile.

Conclusion. We have shown that PI can be considered a SI under a local fields that can break the SI's $\mathbb{Z}_2$ symmetry, and explored some of novel phenomenology which follows, inviting further numerical and experimental analysis. We wish to thank the LDRD office for financial support, and A Libal, C. Reichhardt, CJ Ol-

son Reichhardt (Los Alamos), A. Ortiz and P. Tierno (Barcelona) for sharing preliminary numerical and experimental results. This work was carried out under the auspices of the NNSA of the U.S. DoE at LANL under Contract No. DE-AC52-06NA25396.

[1] J. Bernal and R. Fowler, The Journal of Chemical Physics **1**, 515 (1933).
[2] L. Pauling, Journal of the American Chemical Society **57**, 2680 (1935).
[3] W. Giauque and J. Stout, Journal of the American Chemical Society **58**, 1144 (1936).
[4] A. P. Ramirez, A. Hayashi, R. J. Cava, R. Siddharthan, and B. S. Shastry, Nature **399**, 333 (1999).
[5] G. Möller and R. Moessner, Phys. Rev. B **80**, 140409 (2009).
[6] G.-W. Chern, P. Mellado, and O. Tchernyshyov, Phys. Rev. Lett. **106**, 207202 (2011).
[7] N. Rougemaille, F. Montaigne, B. Canals, A. Duluard, D. Lacour, M. Hehn, R. Belkhou, O. Fruchart, S. El Moussaoui, A. Bendounan, et al., Phys. Rev. Lett. **106**, 057209 (2011).
[8] S. Zhang, I. Gilbert, C. Nisoli, G.-W. Chern, M. J. Erickson, L. O Brien, C. Leighton, P. E. Lammert, V. H. Crespi, and P. Schiffer, Nature **500**, 553 (2013).
[9] L. Anghinolfi, H. Luetkens, J. Perron, M. Flokstra, O. Sendetskyi, A. Suter, T. Prokscha, P. Derlet, S. Lee, and L. Heyderman, Nature communications **6** (2015).
[10] C. Nisoli, V. Kapaklis, and P. Schiffer, Nature Physics **13**, 200 (2017).
[11] R. F. Wang, C. Nisoli, R. S. Freitas, J. Li, W. McConville, B. J. Cooley, M. S. Lund, N. Samarth, C. Leighton, V. H. Crespi, et al., Nature **439**, 303 (2006).
[12] C. Nisoli, R. Moessner, and P. Schiffer, Reviews of Modern Physics **85**, 1473 (2013).
[13] M. J. Morrison, T. R. Nelson, and C. Nisoli, New Journal of Physics **15**, 045009 (2013).
[14] I. Gilbert, G.-W. Chern, B. Fore, Y. Lao, S. Zhang, C. Nisoli, and P. Schiffer, Physical Review B **92**, 104417 (2015).
[15] C. Nisoli, J. Li, X. Ke, D. Garand, P. Schiffer, and V. H. Crespi, Phys. Rev. Lett. **105**, 047205 (2010).
[16] E. Mengotti, L. J. Heyderman, A. F. Rodríguez, F. Nolting, R. V. Hügli, and H.-B. Braun, Nat. Phys. **7**, 68 (2010).
[17] N. Rougemaille, F. Montaigne, B. Canals, A. Duluard, D. Lacour, M. Hehn, R. Belkhou, O. Fruchart, S. El Moussaoui, A. Bendounan, et al., Physical Review Letters **106**, 057209 (2011).
[18] S. Ladak, D. Read, W. Branford, and L. Cohen, New Journal of Physics **13**, 063032 (2011).
[19] W. R. Branford, S. Ladak, D. E. Read, K. Zeissler, and L. F. Cohen, Science **335**, 1597 (2012).
[20] B. L. Le, J. Park, J. Sklenar, G.-W. Chern, C. Nisoli, J. D. Watts, M. Manno, D. W. Rench, N. Samarth, C. Leighton, et al., Phys. Rev. B **95**, 060405 (2017), URL `https://link.aps.org/doi/10.1103/PhysRevB.95.060405`.
[21] A. Farhan, P. Derlet, A. Kleibert, A. Balan, R. Chopdekar, M. Wyss, L. Anghinolfi, F. Nolting, and L. Heyderman, Nature Physics (2013).
[22] V. Kapaklis, U. B. Arnalds, A. Farhan, R. V. Chopdekar, A. Balan, A. Scholl, L. J. Heyderman, and B. Hjörvarsson, Nature nanotechnology **9**, 514 (2014).
[23] J. Porro, A. Bedoya-Pinto, A. Berger, and P. Vavassori, New Journal of Physics **15**, 055012 (2013).
[24] I. Gilbert, Y. Lao, I. Carrasquillo, L. O?Brien, J. D. Watts, M. Manno, C. Leighton, A. Scholl, C. Nisoli, and P. Schiffer, Nature Physics **12**, 162 (2016).
[25] I. Gilbert, C. Nisoli, and P. Schiffer, Physics Today **69**, 54 (2016).
[26] A. Libál, C. Reichhardt, and C. J. Olson Reichhardt, Phys. Rev. Lett. **97**, 228302 (2006).
[27] A. Libál, C. O. Reichhardt, and C. Reichhardt, Phys. Rev. Lett. **102**, 237004 (2009).
[28] C. J. O. Reichhardt, A. Libal, and C. Reichhardt, New Journal of Physics **14**, 025006 (2012).
[29] A. Libál, C. Nisoli, C. Reichhardt, and C. Reichhardt, Physical Review Letters **120**, 027204 (2018).
[30] A. Libál, C. Reichhardt, and C. O. Reichhardt, Physical Review E **86**, 021406 (2012).
[31] A. Libál, C. Nisoli, C. Reichhardt, and C. O. Reichhardt, Scientific Reports **7** (2017).
[32] A. Ortiz-Ambriz and P. Tierno, Nature communications **7** (2016).
[33] J. Loehr, A. Ortiz-Ambriz, and P. Tierno, Physical Review Letters **117**, 168001 (2016).
[34] M. L. Latimer, G. R. Berdiyorov, Z. L. Xiao, F. M. Peeters, and W. K. Kwok, Phys. Rev. Lett. **111**, 067001 (2013).
[35] J. Trastoy, M. Malnou, C. Ulysse, R. Bernard, N. Bergeal, G. Faini, J. Lesueur, J. Briatico, and J. E. Villegas, Nature nanotechnology **9**, 710 (2014).
[36] J.-Y. Ge, V. N. Gladilin, J. Tempere, V. S. Zharinov, J. Van de Vondel, J. T. Devreese, and V. V. Moshchalkov, Physical Review B **96**, 134515 (2017).
[37] R. Baxter, *Exactly solved models in statistical mechanics* (Academic, New York, 1982), ISBN 0120831805.
[38] E. H. Lieb, Physical Review **162**, 162 (1967).
[39] G.-W. Chern, M. J. Morrison, and C. Nisoli, Phys. Rev. Lett. **111**, 177201 (2013).
[40] C. Castelnovo, R. Moessner, and S. L. Sondhi, Nature **451**, 42 (2008).
[41] J. Li, S. Zhang, J. Bartell, C. Nisoli, X. Ke, P. Lammert, V. Crespi, and P. Schiffer, Phys. Rev. B **82**, 134407 (2010).
[42] A. Libal and et al, Submitted (2017).
[43] I. Gilbert, G.-W. Chern, S. Zhang, L. O?Brien, B. Fore, C. Nisoli, and P. Schiffer, Nature Physics **10**, 670 (2014).
[44] J. Drisko, T. Marsh, and J. Cumings, Nature Communications **8** (2017).
[45] J. P. Morgan, A. Stein, S. Langridge, and C. H. Marrows, Nat. Phys. **7**, 75 (2010).